



PII: S0925-7535(97)00028-3

UNCERTAINTY MODELING: EXAMPLES AND ISSUES¹

Roger M. Cooke

Department of Mathematics, Delft University of Technology, Delft, The Netherlands

Abstract—New techniques in uncertainty analysis are illustrated with simplified examples from recent applications of interest for safety science. The applications are: BLEVE (boiling liquid expanding vapor explosions) models, satellite life distributions, dispersion coefficients and modeling contamination in food chains. The examples illustrate the importance of carefully modeling dependence in uncertainties. They also illustrate new uses of conditional Monte Carlo sampling. © 1997 Elsevier Science Ltd.

1. Introduction

The last few years have seen many new developments in the field of uncertainty analysis. Decision makers are increasingly demanding some defensible representation of uncertainty surrounding the output of complicated mathematical models. Scientists in turn are putting more effort into the modeling and propagation of uncertainty. To illustrate the effect of these developments Fig. 1 shows two representations of uncertainty in peak (center line) concentration as a function of down wind distance, following an airborne release of toxic material. The KfK picture is representative of uncertainty analyses done informally with in-house experts (Fischer et al., 1990). The CEC \ NRC picture is based on formal expert judgment methods and more rigorous uncertainty modeling (Cooke et al., 1994).

From a mathematical perspective uncertainty analysis is concerned with determining the uncertainty in the output of a mathematical model, relative to an assessment of the uncertainty of the model's input. The model may be a simple algebraic sum or a complicated set of equations and numerical procedures. It is only essential that the model is written as a mathematical function of some vector of arguments:

$$\text{Model: } M(X_1, \dots, X_n).$$

The variables X_1, \dots, X_n are assumed to take real values, and M is a function returning a real vector. In practice we may be able to write down a mathematical model describing a given

¹ Originally published in SRD Association Members Conference 1994 "Corporate Responsibility and Regulation" 5/6–10–94, Warrington, UK.

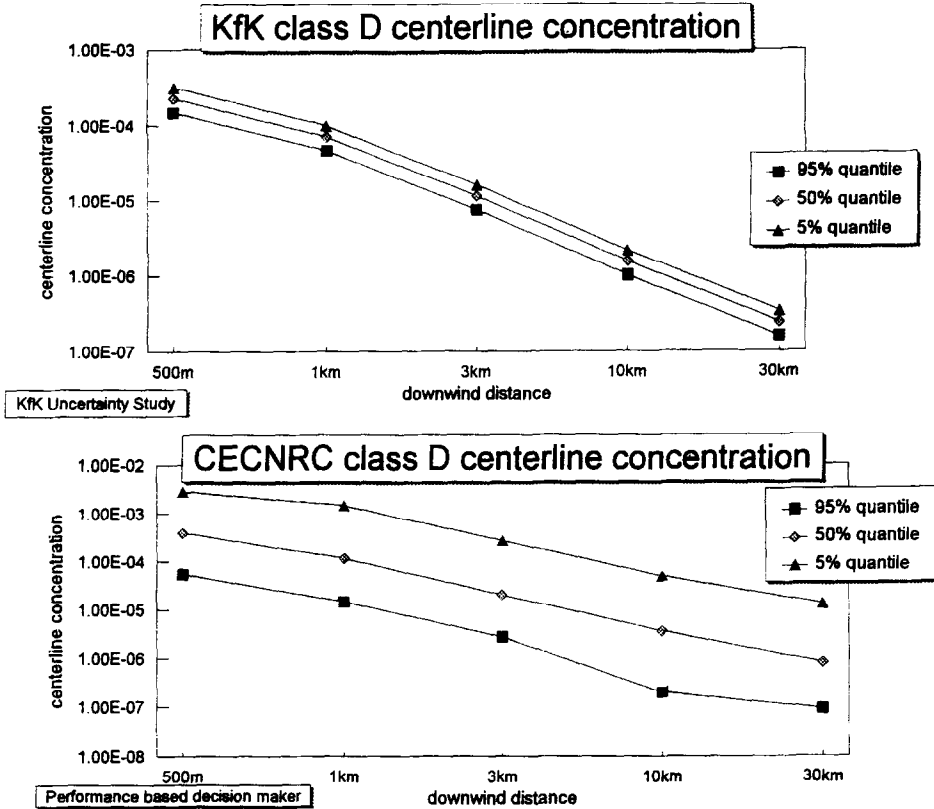


Fig. 1. KfK and CECNRC predictions for centerline concentration.

problem, but may be unable to obtain a numerical answer because we don't know the values of the arguments. In such situations we must assess the uncertainty in the input variables X_1, \dots, X_n . In uncertainty analysis the variables X_1, \dots, X_n are considered as random variables. The joint probability distribution of X_1, \dots, X_n describes the uncertainty over the input of the model M . In uncertainty analysis this joint distribution is pushed through the model M to yield an uncertainty distribution on the model's output.

This paper provides an introduction to uncertainty analysis by stepping through some examples chosen from real studies performed at the Department of Mathematics, Delft University of Technology. They are intended to illustrate new issues and techniques of uncertainty analysis, including dependence modeling, the use of latent variables, post-processing and conditional sampling. These cases were all analysed with the PC system UNICORN (UNcertainty analysIs with CORrelatioNs) developed at the Delft University of Technology (Cooke, 1995).

2. Examples of uncertainty analysis

The first example is a rather straightforward application of uncertainty analysis of a type of explosion model used in citing and licensing decisions. In second example uncertainty analysis

with dependence is used to evaluate the reliability of a satellite system where traditional methods (without uncertainty analysis) would not work. The third and fourth examples deal with ‘post-processing’ experts’ uncertainty assessments to transfer uncertainty from an observable domain onto the parameter space of some model.

2.1. Effects of a BLEVE

A BLEVE (Boiling Liquid Expanding Vapor Explosion) results when a pressurized propane storage tank bursts. A fireball forms, rises to a certain height and burns. The main risk contributor from a BLEVE is the heat radiated in the first 20 s. The Dutch government uses the following formula to compute the heat radiation at ground distance x from the storage tank, received during 20 s from the center of the fireball:

$$q(x) = \frac{50\,000\tau(r)\delta_1 P^{\delta_2} M * 20}{4\pi r^2 t} \text{ (kJ/m}^2\text{)},$$

where P = pressure of propane prior to release (10^6 Pascal); M = mass of propane (kg); t = burn time = $\beta_1 M^{\beta_2}$ (s); $\tau(r)$ = transmissivity of radiated heat through air, = $\min\{1, 1.385 - 0.135 \log(rPw)\}$; Pw = humidity of air (Pascal); D = diameter of fireball = $\alpha_1 M^{\alpha_2}$ (m); h = height of fireball = γD (m); $r = (x^2 + h^2)^{1/2}$.

A reference accident was chosen using $M = 10^6$ kg, $P = 840\,000$ Pa. Values for the other constants can be retrieved from the literature. However, the spread of published values is rather large. The Dutch consulting firm AVIV performed an uncertainty analysis on the BLEVE model; TU Delft provided comments on the AVIV study. The numbers shown in Table 1 were taken from AVIV (1986) (see also Meeuwissen and Cooke, 1989).

$q(x)$ is the main risk indicator in licensing decisions; first degree burns appear at $q = 113$ kJ/m². Fig. 2 shows $q(x)$ for $x = 1000$ to 2000 m for the reference accident. Three curves are shown, corresponding to the nominal, most optimistic and most pessimistic values for the parameters in $q(x)$. The spread is quite large. For $x = 1000$ m, the most optimistic value is about 100 kJ/m, the nominal value is 200 kJ/m and the most pessimistic value is 3600 kJ/m.

Figure 2 does not provide a realistic representation of the uncertainty in the BLEVE model, as it is quite unlikely that all uncertain parameter values would take their most optimistic or most pessimistic values.

Table 1
Values for constants in BLEVE model

	α_1	α_2	β_1	β_2
Fay, Lewis	6.36	0.333	2.57	0.167
Hardee	6.24	0.33	1.11	0.167
Hasegawa, Sato (1)	5.28	0.277	1.099	0.097
Hasegawa, Sato (2)	5.25	0.314	1.07	0.181
Gayle, Branford	6.14	0.325	0.41	0.34
Moorhouse	5.33	0.327	0.923	0.303
Roberts	5.8	0.333	0.45	0.333
TNO 1983	6.48	0.325	0.852	0.26

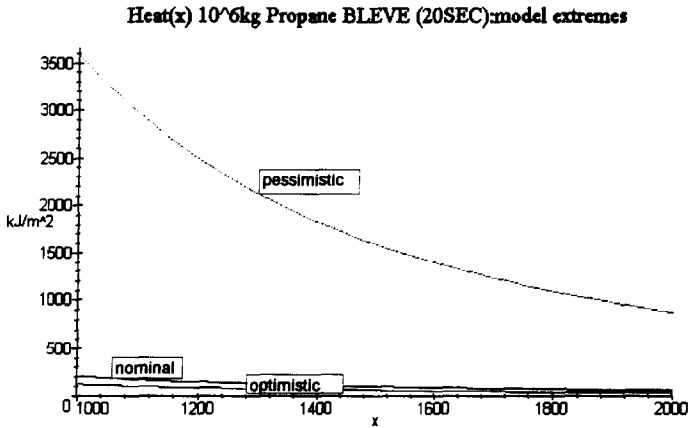


Fig. 2. Optimistic, nominal and pessimistic scenarios.

AVIV developed a response surface linearized approximation to $q(x)$ and assigned distributions based on published values to the parameters α_1 , β_1 , γ , δ_1 and P_w . Other parameters were held constant at their nominal values. Sampling independently from these distributions a distribution for $q(x)$ was generated. The exponents α_2 and β_2 were treated as constants. Although Table 1 exhibits a spread of values for these exponents, it would be unreasonable to sample these independently of the values for α_1 , resp. β_1 .² TU Delft performed an uncertainty analysis of the unlinearized $q(x)$ under the AVIV assumptions, and also under alternative assumptions. According to the alternative assumptions, α_2 and β_2 were assigned distributions which were correlated with α_1 resp. β_1 , based on the data in Table 1 (Meeuwissen and Cooke, 1989). In the TU Delft study it emerged that β_2 , affecting the total burn time was the most sensitive parameter for $q(x)$.

Figure 3 shows 5% and 95% confidence bounds for $q(x)$, $x = 1000, 1500, 2000$ (without linearization), using the AVIV and the alternative assumptions on the uncertainty of the parameters in $q(x)$. Figures 2 and 3 draw attention to the importance of carefully modeling uncertainty, with dependence, in using quantitative models with uncertain parameters to support siting and licensing decisions. The 95% quantile for the main risk indicator at 1000 m varies by more than an order of magnitude over the three figures.

2.2. Cluster

The Cluster mission at the European Space Agency involves simultaneously launching four identical satellites to measure turbulence in the cusp of the earth's magnetic field. The four satellites must orbit in a rigid tetrahedral configuration and must pass through the cusp several times to accomplish all the mission goals. The design life for each satellite is 2 years

² From dimensional analysis assuming that q is a function of the quantities listed above, it can be derived that $\alpha_2 = 0.333$, $\beta_2 = 0.333$. These are NOT the nominal values used in the AVIV study (0.327 and 0.303 respectively). Moreover, this argument neglects other forces, e.g. buoyancy forces in the atmosphere, which would lead to very different values.

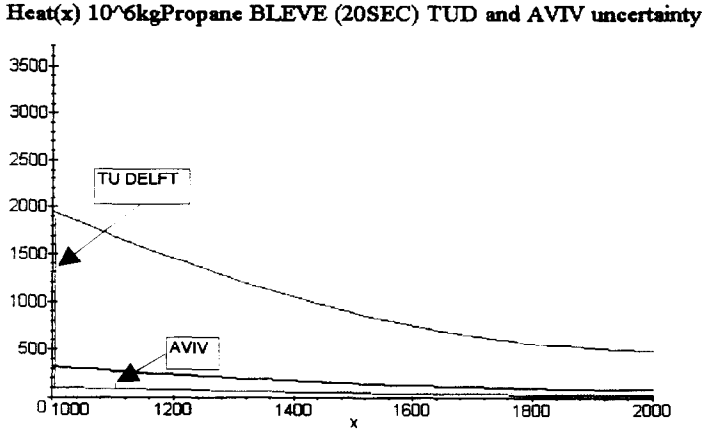


Fig. 3. TU Delft and AVIV uncertainty bounds.

(720 days). During the design phase, a cursory traditional reliability analysis was performed for a single satellite, and it emerged that the probability of surviving at least 720 days was about 0.80. Since mission success required the functioning of all four satellites for 720 days, the traditional analysis, treating the satellite lifetimes as independent random variables, predicted a mission success probability of $(0.80)^4 = 0.41$. This figure was alarmingly low. If this cursory analysis were correct, project management would have to contemplate design enhancements, possibly involving a 5th redundant satellite, before moving forward.

The TU Delft was asked to review this cursory analysis to determine whether it could be enhanced prior to committing additional resources to improve data and possibly to change design. The TU Delft analysis was published at the ESREL '95 Conference (Bedford and Cooke, 1995). A simplified account of the main findings is described here.

Two features of the traditional reliability analysis were identified as unrealistically pessimistic. Neither could be redressed with traditional calculational methods, and both were treated simply with UNICORN. First, on the traditional analysis no credit could be given for partial completion of mission goals. If one satellite expired on day 719 while the others were still functioning, this would count as mission failure. In discussions with project management it emerged that, roughly speaking, 80% of the mission goals would be realized if four satellites survived for 180 days and at least three survived for two years. The second unrealistic feature of the traditional analysis was that the four satellites were assumed to be independent. This however is quite unrealistic. The four satellites are built by the same contractor to identical specifications, launched together and subject to the same stresses during passage through the earth's shadow. In so far as these factors contribute to failure, the lifetimes should be modeled as positively dependent. Intuitively speaking, if one satellite fails 'sooner than expected' then knowledge of this fact should increase our assessment of the probability that the others also fail sooner than expected.

2.2.1. The traditional analysis

The traditional analysis modeled the cluster system as the minimum of four independent identically distributed life variables with constant failure rate of $\lambda = 0.00031/\text{day}$. Since the

failure rate of the minimum of independent exponentials is the sum of the individual failure rates, a system failure rate of 0.00124/day resulted. Hence

$$P(\text{minimum of four satellites lives longer than 720 days}) = e^{-0.00124 * 720} = 0.41.$$

2.2.2. Partial mission success

To compute the probability that at least 80% of the mission goals are realized, we must compute

$$P(\text{all four satellites} \geq 180 \text{ and at least three} \geq 720).$$

On the assumption of independence this can be done analytically but the computation is tedious. It can be simulated quite easily with generalized indicator functions:

$$ik\{A, X_1, \dots, X_n, B\} = \begin{cases} 1 & \text{if at least } k \text{ of } X_1, \dots, X_n \text{ are between } A \text{ and } B, \\ 0 & \text{otherwise.} \end{cases}$$

A and B may be random variables but in this case we treat them as constants. If X_1, \dots, X_4 represent the lifetimes of the four satellites the probability can be simulated by simulating the distribution of

$$i1\{180, \min(X_1, X_2, X_3, X_4), \infty\} * i3\{720, X_1, X_2, X_3, X_4, \infty\}.$$

Sampling 1000 times independently from the distributions of $X_i, i = 1, \dots, 4$, the probability of the event in question from simulated is 0.69.

2.2.3. Dependence

The assumption of independence is pessimistic, this can be seen intuitively as follows. If the four satellites were completely dependent, then the probability that they all four fail before time T is equal to the probability that one of them fails before T . If they are independent, then the probability that one of the four fails before T is greater. It is not clear what value of dependence should be used but a rather strong positive coupling is more realistic than the assumption of independence. The simulation was done for a number of rank correlations between the satellite's life distributions (an explanation of rank correlation is given below). Using a rank correlation of 0.75 between all four satellites yielded the following comparison to the case of independence: The probability of realizing at least 80% of the mission goals rose from 0.69 to 0.72; and the probability that all four satellites functioned at least 720 days rose from 0.41 to 0.64.

Figures 4 and 5 show the reliability of the 4 out of 4 system and the 4 out of 5 system with different values for the correlation in satellite life times.³ On the basis of such calculations, project management decided to proceed to the next phase without redesigning the satellites or re-configuring the missions.

³ The satellite distributions used here were modeled using competing risk models for different stresses during mission; they were not modeled with constant failure rates as in the simplified example discussed here.

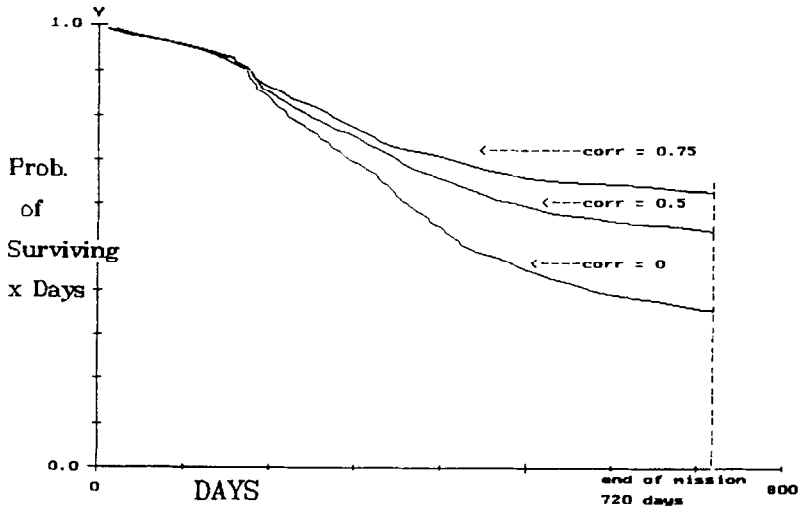


Fig. 4. Cluster reliability (4 out of 4) with correlations.

2.3. Post-processing expert uncertainty assessments

The following examples are representative of new types of applications of uncertainty analysis. To perform uncertainty analysis of large computer models, uncertainty distributions are placed on the model's unknown parameters. If the parameters have a straightforward empirical interpretation, then distributions can be developed directly, either with observational data or expert judgment. Often however, the model's parameters do not possess a transparent and straightforward empirical interpretation. The option of obtaining distributions from data is excluded. Expert judgment is sanctioned if experts are queried only about *observable* (not necessarily observed) phenomena. ⁴ 'Post-processing' denotes the method or methods used in projecting the elicited distributions over physical quantities onto the parameters space of a model.

2.3.1. Post-processing dispersion coefficients

The first example was developed in the course of the joint CEC \ USNRC uncertainty study (Cooke, 1994; Cooke et al., 1994; Harper et al., 1994). Uncertainty distributions were required for the coefficients in the power law expressions for cross wind dispersion $\sigma_y(x, sc)$ and vertical dispersion $\sigma_z(x, sc)$ as a function of down wind distance x and atmospheric stability class.

⁴ This standpoint is crucial for the approach to uncertainty analysis elaborated in (Harper et al., 1994).

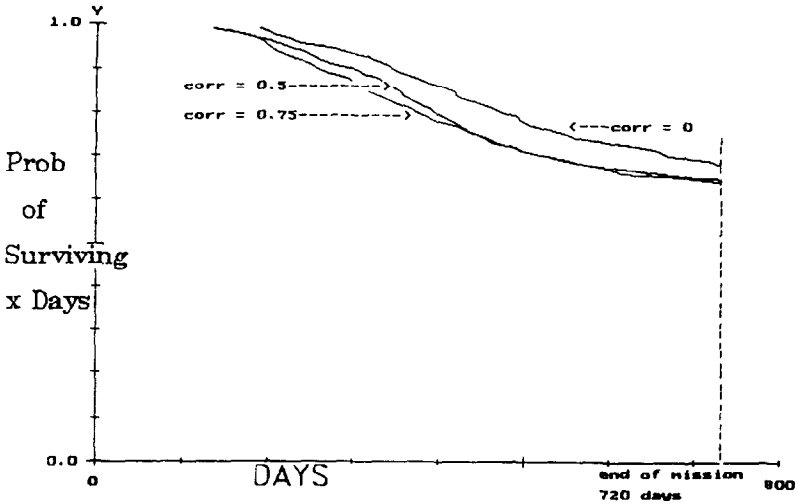


Fig. 5. Cluster reliability (4 out of 5) with correlations.

$$\sigma_y(x, sc) = A_{y,sc} x^{B_{y,sc}},$$

$$\sigma_z(x, sc) = A_{z,sc} x^{B_{z,sc}}.$$

All models for accident consequences following airborne releases incorporate these or similar laws for down wind dispersal. The coefficients A , B are determined per stability class from measured data. The measurements have a fairly low reproducibility and are influenced by a host of factors not included in the model. Therefore, the actual values used in the accident consequence models are uncertain. We focus on $\sigma_y(x)$ and drop the subscripts so that

$$\sigma_y(x) = Ax^B.$$

To quantify the uncertainty on σ_y as a function of down wind distance x , we require a joint distribution on (A, B) . It is hardly reasonable to expect that A and B will be independent. Moreover, the power law is not derived from underlying physical laws, but represents a mere statistical fit to data. The coefficients are not directly measurable.

For all these reasons it was deemed infeasible to query experts about the values of (A, B) directly. Instead, a number of distances $x_1 = 500$ m, $x_2 = 1000$ m, ..., $x_5 = 30$ km were selected and the experts were asked to quantify their uncertainty on σ_y at each of these distances. This distributions for $\sigma_y(x_1), \dots, \sigma_y(x_5)$ were then 'lifted' up to the parameter space of the model. This lifting process will not be described in detail, Fig. 6 gives the basis. It is helpful to transform the power law by taking logs:

$$\log \sigma_y(x_2) = \log A + B \log x.$$

A point (A, B) in the parameter space is mapped onto a line in the observable space $(\log \sigma_y, \log x)$ with slope B . The experts distributions for $\sigma_y(x_i)$ are represented as dotted lines. The probability for the point (A, B) is determined by the probabilities of the points Ax_i^B .

Figure 7 shows a distribution on the parameter space which has been lifted in this way from the observable space. Note that the A and B are strongly correlated in this lifted distribution.

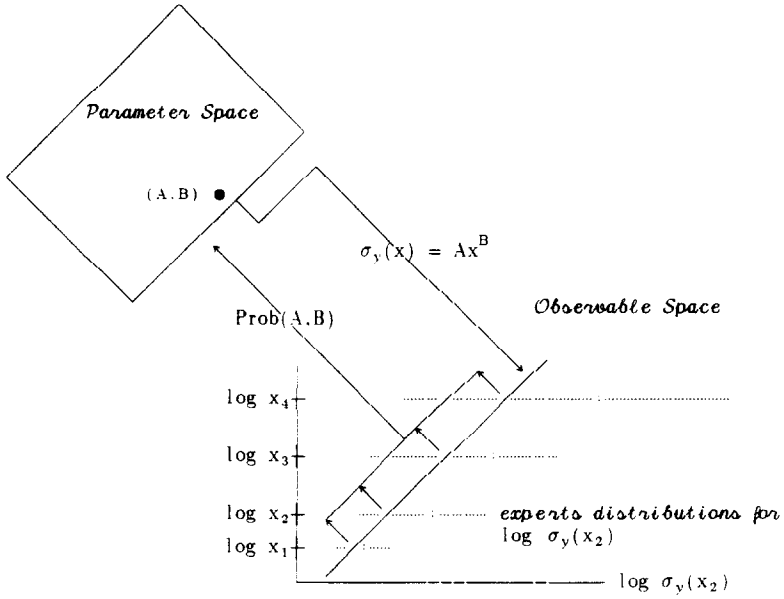


Fig. 6. Schematic for lifting distributions from observable space to parameter space.

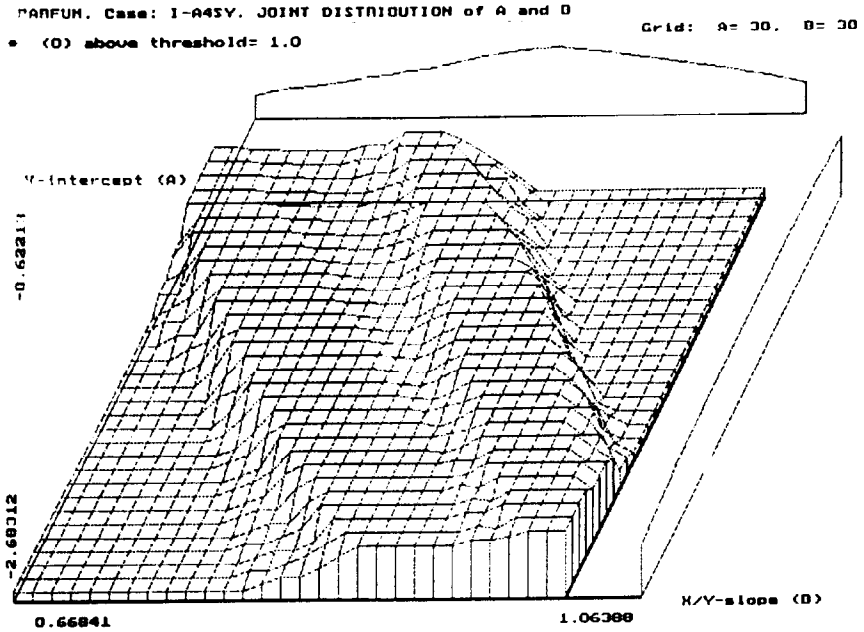


Fig. 7. Joint distribution of power law parameters A, B.

in this way a dependent distribution is induced on the parameter space of the model while the experts are queried only about the outcomes of possible physical measurements.

2.3.2. Post-processing soil migration transfer coefficients

A recurrent problem in assessing uncertainty in physical models is this: We can obtain *marginal* uncertainty distributions on quantities X_1, \dots, X_n . However we know that certain combinations of the X_i are physically impossible. The conditions describing physically possible combinations are complicated and cannot be incorporated easily into the joint distribution over the X_i . We solve this problem by conditional sampling: we sample independently from the marginals, and retain only those samples which satisfy the stipulated conditions. Among all distributions concentrated on physically possible combinations, the conditional distribution thus obtained is the distribution which is ‘closest’ (in the sense of relative information) to the initial distribution. Although the original distributions were independent, after conditionalization the distributions become correlated. Thus, conditional sampling relieves the experts of the task of assessing the correlations themselves. The marginals of the conditional distribution, however, will not coincide with the initial marginals.

Conditional sampling can be extended to impose a probabilistic rather than a deterministic condition. A probabilistic condition may be a distribution supplied by an expert on some function of underlying variables. A pull-back algorithm finds a distribution over the arguments of the function which reproduces the expert’s distribution on the function.

We illustrate this technique with an example from an ongoing uncertainty analysis of food chain models. Consider a model describing the transport of radioactive material through soil following a large airborne release. Modelers construct box models to describe the transport through different soil segments and assign values to the transfer coefficients. A box model of this type is pictured below.

It may take up to 100 years for an initial deposit of radioactive material in box 1 to migrate through to box 5. The values for the transfer coefficients k_{ij} are fitted by oculation (eyeballing) to scant and ambiguous data from concentration measurements at various times following various releases at various places. The point values actually used in the models are therefore characterized by large uncertainties. An uncertainty analysis requires distributions over the transfer coefficients.

A box model like that in Fig. 8 is a picture of a system of first order differential equations with constant coefficients. The coefficient k_{23} for example, describes the proportion of the material in box 2 that moves to box 3 in a small time interval. When no arrow is drawn between two boxes, the proportion moved between these boxes is zero. Transfer coefficients and amounts of material are always positive. In this application, as in most applications of such models, the transfer coefficients cannot be measured directly.

Given such a system with fixed values for the transfer coefficients, we can solve for the functions $m_i(t)$ = amount in box i at time t , as follows:

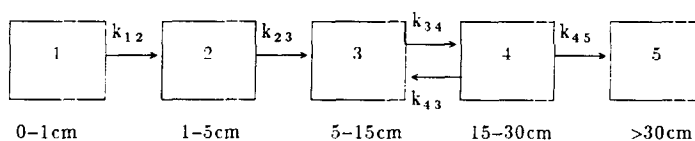


Fig. 8. Box model for soil migration.

1. Extract the eigenvectors from the coefficient matrix $K = \{k_{ij}\}$, setting $k_{ij} = 0$ when no arrow is indicated.
2. Form a basis of solutions using the eigenvectors and eigenvalues of K , as described in any textbook on differential equations.
3. Express the initial mass distribution at time $t = 0$ as a linear combination of the basic solutions from step 2.

For example, under the initial condition: $m_1(0) = 1$, $m_j(0) = 0$, $j = 2, \dots, 5$: we have for the first two boxes:

$$m_1(t) = e^{-tk_{12}},$$

$$m_2(t) = \frac{k_{12}(e^{-tk_{23}} - e^{-tk_{12}})}{k_{12} - k_{23}}.$$

Experts are reluctant to assess uncertainty over the transfer coefficients. Their knowledge is best expressed in uncertainty distributions over the time T_i at which half the total material passes through box i : that is $m_1(T_i) + m_2(T_i) + \dots + m_i(T_i) = 1/2$. Let \mathcal{F}_1 and \mathcal{F}_2 denote random variables having the expert's assessed distributions for the half-lives T_1 and T_2 (\mathcal{F}_1 and \mathcal{F}_2 are assumed independent, but this is not essential). We want to use these in conjunction with the above equations to obtain a joint distribution on (k_{12}, k_{23}) . This can be done with an appropriate use of conditional sampling. The following brief description is intended to show the rough contours of the method. We confine attention to T_2 .

The method involves the following mathematical fact: If X and Y are independent random variables taking outcomes in $\{1, \dots, n\}$, then the distribution of X conditional on $X = Y$ is equal to the unconditional distribution of Y if, and only if, X is uniform.

Using \mathcal{F}_1 in the first equation above, we obtain immediately the distribution for k_{12} as $\ln(2)/\mathcal{F}_1$. Using numerical interpolation, we may write T_2 as a function of k_{12} and k_{23} . Let us assume an *arbitrary* independent distribution for k_{23} , independent of k_{12} and \mathcal{F}_2 . Sample from $(k_{12}, k_{23}, \mathcal{F}_2)$, compute $T_1 (= \ln(2)/k_{12})$ and T_2 (a function of k_{12}, k_{23}) and retain the sample only if the following condition C holds

$$C: G(T_2) = G(\mathcal{F}_2)$$

where G transforms T_2 into a uniform variable. It can be shown that conditional on C, T_2 has the distribution of \mathcal{F}_2 , and the variables k_{12} and k_{23} will be correlated. Moreover the result depends on the arbitrary choice for the distribution of k_{23} . Unless further information is available, it is advisable to choose the initial distribution of k_{23} to be non-informative over the range of all physically plausible values.

3. Conclusions

Examples have been given to illustrate how uncertainty plays a role in framing complex decision problems. Mathematical techniques are available to propagate correlated uncertainties through complicated models. Conversely, we can use assessments of uncertainty over observable target variables to induce distributions over unobservable variables. The numerical results given here show that dependence cannot be neglected in real problems.

References

- AVIV (1986) *The Uncertainty in Consequence Calculations in Risk Studies*. Enschede, The Netherlands.
- Bedford, T. and Cooke, R. (1995) Achievement assessment for the Cluster project. In *Proceedings ESREL95, Bournemouth, June 26–28*. pp. 123–149.
- Cooke, R. (1994) Parameter fitting for uncertain models; modelling uncertainty in small models. *Reliability Engineering and System Safety* **44**, 89–102.
- Cooke, R. (1995) *UNICORN: Methods and Code for Uncertainty Analysis*. Published by AEA Technology for the European Safety and Reliability Association, Cheshire.
- Cooke, R. Goossens, L. and Kraan, B. (1994) *Methods for CC\USNRC Accident Consequence Uncertainty Analysis of Dispersion and Deposition*. EUR.15856 EN.
- Fischer, F. Ehrhardt, J. Hasemann, I. (1990) *Uncertainty and Sensitivity Analysis of the Complete Program System UFOMOD and Selected Submodels*. Kernforschungszentrum Karlsruhe, KfK 4627.
- Harper, F. Goossens, L. Cooke, R. Hora, S. Young, M. Päsler-Ssauer, J. Miller, L. Kraan, B. Lui, C. McKay, M. Helton, J. Jones, A. (1994) *Joint USNRC\CC consequence Uncertainty Study: Summary of Objectives, Approach, Application, and Results for the Dispersion and Deposition Uncertainty Assessment*, Vol. III. EUR 15755 EN, SAND94-1453.
- Meeuwissen, A. and Cooke, R. (1989) Uncertainty analysis of the accident effect area of a BLEVE. (Report No. 89-49).: Department of Mathematics, Delft University of Technology Delft.